

Amperometric sandwich immunoassay for the carcinoembryonic antigen using a glassy carbon electrode modified with iridium nanoparticles, polydopamine and reduced graphene oxide

Luyang Miao¹ · Lei Jiao¹ · Juan Zhang¹ · He Li¹

Received: 23 July 2016 / Accepted: 1 November 2016 / Published online: 8 November 2016
© Springer-Verlag Wien 2016

Abstract The authors describe a sandwich-type electrochemical immunoassay for sensitive determination of the carcinoembryonic antigen (CEA). It is based on the use of iridium nanoparticles (Ir NPs) acting as electrochemical signal amplifier on the surface of a glassy carbon electrode. At first, polydopamine-reduced graphene oxide (PDA-rGO) was employed to immobilize primary antibody (Ab₁) against CEA. Secondly, Ir-NPs were used as a support for the immobilization of secondary antibody (Ab₂) to afford signal labels. The large surface area of PDA-rGO and the excellent electro-oxidative H₂O₂-sensing properties of Ir NPs result in a sensitive assay for CEA. Operated best at a working voltage of -0.6 V (vs. SCE), the assay has a linear range that extends from $0.5 \text{ pg}\cdot\text{mL}^{-1}$ to $5 \text{ ng}\cdot\text{mL}^{-1}$, and the lower detection limit is $0.23 \text{ pg}\cdot\text{mL}^{-1}$. The immunosensor displays satisfactory reproducibility and stability, thus demonstrating a reliable immunoassay strategy for tumor biomarkers. It was applied to the determination of CEA in spiked serum samples.

Keywords Immunosensor · Sandwich-type · Tumor biomarker · Immobilization · Electrochemical signal amplification · Electrochemical impedance spectroscopy · Hexacyanoferrate · Nyquist plot · Hydrogen peroxide · Serum analysis

Electronic supplementary material The online version of this article (doi:10.1007/s00604-016-2010-5) contains supplementary material, which is available to authorized users.

✉ He Li
lihecd@gmail.com

¹ School of Chemistry and Chemical Engineering, and School of Biological Science and Technology, University of Jinan, Jinan 250022, China

Introduction

The carcinoembryonic antigen (CEA) is a reliable serum biomarker in case of colorectal cancer, breast cancer and lung cancer [1–3]. Thus, it is urgently necessary to precisely detect CEA in fields of modern biomedicine and clinical diagnostics. Conventional immunoassays such as enzyme-linked immunosorbent assays (ELISA) [4], chemiluminescence immunoassays [5], radioimmunoassays (RIA) [6] and electrochemical immunoassay [7] have been used for detecting CEA. Among them, electrochemical immunoassay has attracted more and more attention by virtue of simple operation, high sensitivity and cost-effectiveness [8–10].

Sandwich-type immunosensor, binding of highly specific antigens with antibodies (Ag-Ab) and then reacting with secondary antibodies which are combined as a label for signal amplification, has become one of popular analytical techniques in biomedical analysis, food quality testing and environmental monitoring [11–13]. In contrast with label-free immunosensor, there is no denying that sandwich-type immunosensor has unique charm that can yield larger signals, the higher sensitivity, the lower detection limit, and the avoidance of interferences by sample impurities [14]. Furthermore, the emerging of different type nanomaterials has brought an enormous opportunity to sandwich-type immunosensor, including carbon nanotubes [15], oxide nanomaterials [16], metal nanoparticles [17] and nanocomposite [18, 19]. Such immunosensors based on nanomaterials show good performance that preserves the bioactivity of antibodies and enhance electrochemical properties of the immunosensors, for instance, fast electron transfer and high signal to noise ratio (S/N) [20, 21].

It is well known that sandwich-type electrochemical immunosensor strongly relies on signal labels to transduce and amplify the signal change resulted from the bio-recognition process of analytes [22]. Therefore, the sensitivity of sandwich-type electrochemical immunosensor depends on the signal amplify strategy. Owing to the inherited features of high specific reactivity towards the substrate, natural enzymes become the most commonly used signal amplification labels for sensitive electrochemical immunoassay, such as horseradish peroxidase was widely used to fabricate electrochemical signal labels by virtue of the high electrochemical reduction towards hydrogen peroxide [23, 24]. However, the catalytic activity of natural enzyme is more easily influenced by the external surroundings such as pH value and temperature. Alternatively, nanomaterials possessed high electrochemical reduction activities on hydrogen peroxide were adopted to prepare signal labels for sensitive detection of tumor biomarkers [22]. Iridium nanoparticles (Ir NPs) have received considerable attention in the field of fluorescence labeling [25], catalytic synthesis [26], sensing [27] and so on. Among the various transition metals, Ir NPs have been considered as an excellent catalysis due to the inherited high selectivity and stability, especially large surface area and high density of active sites [28, 29]. Based on these merits, Ir NPs are fitting well as signal labels for the fabrication of electrochemical immunosensors.

Herein, we utilized the unique sandwich-type electrochemical immunosensor based on Ir NPs and polydopamine-reduced graphene oxide (PDA-rGO) for sensitive detection of CEA. The high sensitivity was implemented by using the large surface area of PDA-rGO to increase the amount of immobilized Ab₁, and its high conductivity. Furthermore, Ir

NPs as signal tags of the immunosensor have excellent catalase-mimic performance, large surface area and good dispersion, revealing the promising application for developing electrochemical immunosensors.

Experimental section

Equipment

Scanning electron microscopy (SEM) images were recorded using a COXEM EM-30 Plus (Korea). Transmission electron microscope (TEM) images were obtained on a Philips CM200 UT (Field Emission Instruments, USA). Fourier transform infrared (FT-IR) spectra were acquired by Perkin-Elmer 580B spectrophotometer (Perkin-Elmer, USA). Three-electrode device including a glassy carbon electrode (GCE), a saturated calomel electrode (SCE) and a platinum-wire electrode was used for electrochemical measurements. All electrochemical detections were performed by a CHI 760D workstation (China).

Reagents and materials

Graphite powder (99.95%) and Bovine serum albumin (BSA, 96–99%) was purchased from Shanghai Macklin Biochemical Technology Co., Ltd. (<http://www.macklin.cn/>). Iridium chloride hydrate (IrCl₃, 99.9%) was bought from Alfa Aesa (<https://www.alfa.com/zh-cn/>). The carcinoembryonic Antigen (CEA) and paired antibody were obtained from Shanghai Linc-Bio Science Co., Ltd. (<http://linc-bio.cn/>). All the other reagents were analytical grade and used directly

Scheme 1 The fabrication process of the electrochemical immunosensor

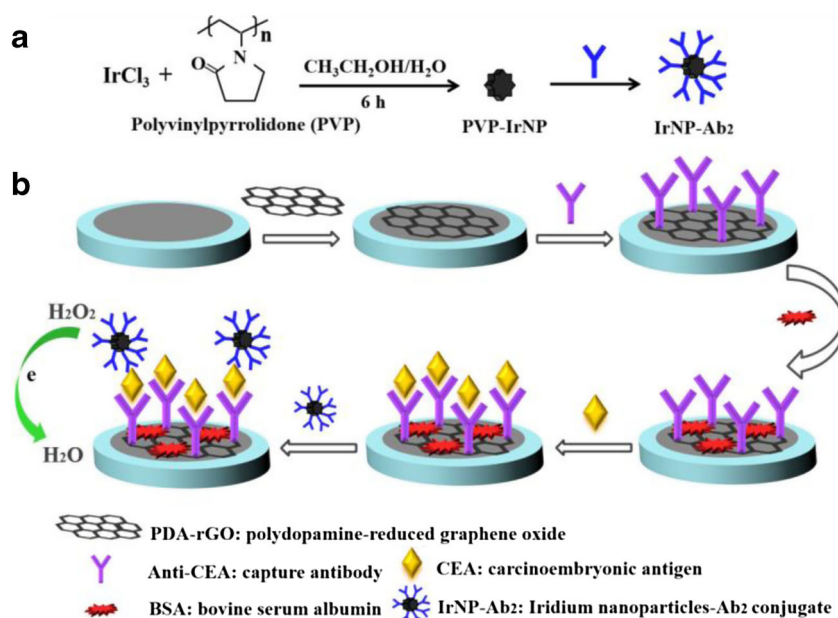
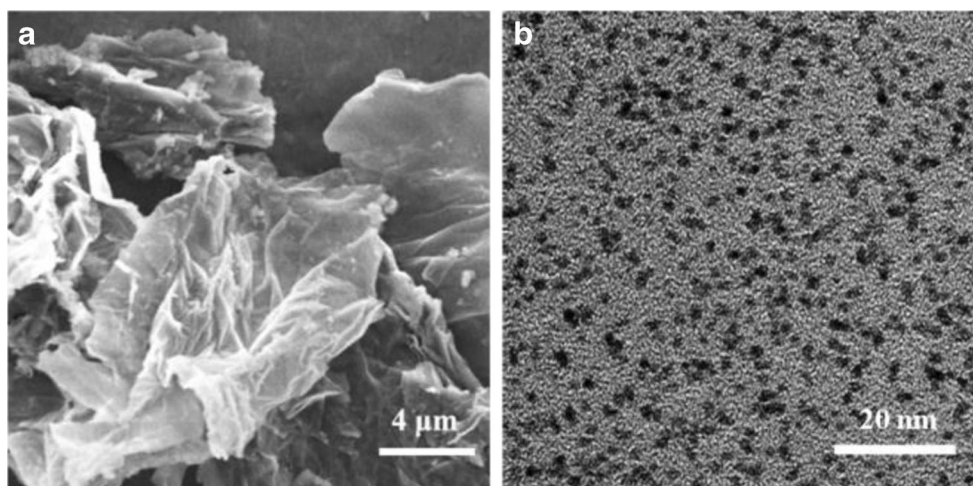


Fig. 1 SEM image of PDA-rGO **a** and TEM image of PVP-Ir NPs **b**



without further treatments. Ultrapure water was utilized throughout the experiments.

Preparation of PDA-rGO

Polydopamine-reduced graphene oxide (PDA-rGO) was prepared following the reported procedure [30]. Dopamine (20 mg) was added to 10 mL, 10 mM of Tris-HCl buffer (pH 8.5), and then mixed with $1.0 \text{ mg}\cdot\text{mL}^{-1}$ GO. The mixture was stirred for 24 h at 25°C . Thereafter, PDA-rGO was obtained after centrifuging and washing twice with ultrapure water.

Preparation of PVP-Ir NPs

Polyvinylpyrrolidone-stabilized colloidal Iridium nanoparticles (PVP-Ir NPs) were prepared by an ethanol reduction approach [31]. A representative synthesis procedure can be described as follows: aqueous IrCl_3 solution ($8.4 \mu\text{mol}$, 4 mL) was slowly dropped into 4 mL of ethanol solution containing PVP ($168 \mu\text{M}$), then the mixture was stirred vigorously at 25°C for 12 h before the pale yellow solution appeared. The solution

was refluxed in air at 100°C for 6 h until the brown solution was obtained. Finally, PVP-Ir NPs were obtained by subsequent evaporating process and then the black products were dispersed in phosphate buffer (0.1 M, pH 7.4), and stored at 4°C .

Preparation of Ir NPs- Ab_2 as labels

1 mL of PVP-Ir NPs ($3 \text{ mg}\cdot\text{mL}^{-1}$) was mixed with 1 mL of Ab_2 ($200 \text{ ng}\cdot\text{mL}^{-1}$), the mixture was placed at an oscillator for incubating Ab_2 under 4°C for 12 h. The labels of Ir NPs- Ab_2 were obtained by centrifuging and washing with phosphate buffer. Finally, the resulting labels were redispersed in phosphate buffer including 1% (m:m) BSA and stored at 4°C before use.

Procedures

As illustrated in Scheme 1, a sandwich-type electrochemical immunosensor was constructed. Firstly, a working electrode GCE was polished by alumina powders affording a mirror-like surface. $6 \mu\text{L}$ of well-dispersed PDA-rGO ($1.5 \text{ mg}\cdot\text{mL}^{-1}$) was dropped on the pretreated GCE and dried out. Then $6 \mu\text{L}$ of primary CEA antibody (Ab_1 , $200 \text{ ng}\cdot\text{mL}^{-1}$) was coated on the electrode through the ability of PDA enabling protein conjugation. After drying, 1% BSA solution was dropped on the electrode for incubating 1 h at 37°C to block the nonspecific sites. Consequently, CEA with given concentration was added on the modified electrode. Finally, $6 \mu\text{L}$ of Ir NPs- Ab_2 was added for incubating 1 h at 37°C . After that, the modified electrode was ready for electrochemical measurement.

The measurement parameters of cyclic voltammograms (CV) are listed as follows: (a) potential range, -1.0 to 0.6 V ; scan rate, 0.1 V/s . The electrochemical-impedance spectra (EIS) was assayed from 1 to 10^5 Hz with an amplitude of 5 mV in $5.0 \text{ mM Fe}(\text{CN})_6^{3-/4-}$ solution containing 0.1 M KCl . The operating potential of amperometric detection is -0.6 V due to the largest redox current appears here, and run time is 200 s.

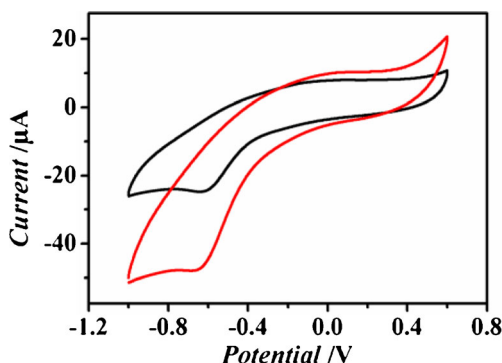
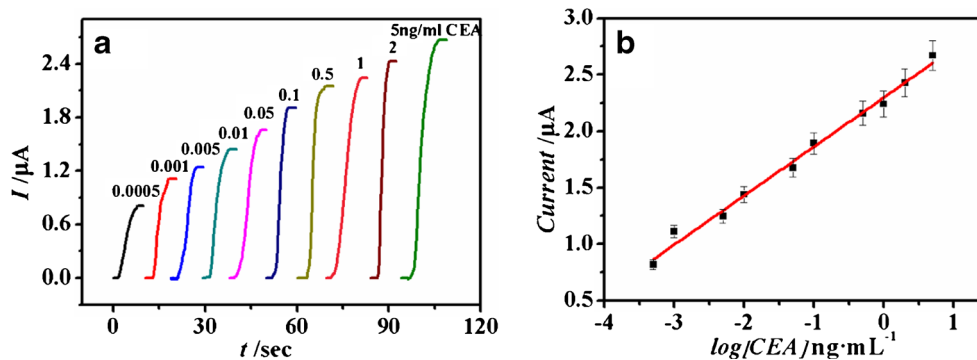


Fig. 2 Cyclic voltammograms of Ir NPs modified electrode in phosphate buffer in the absence (black) and presence (red) of $5 \text{ mM H}_2\text{O}_2$

Fig. 3 Amperometric response **a** and calibration curve **b** of the immunosensor about different CEA concentrations. Error bar = RSD ($n = 5$)



Results and discussion

Choice of materials

Graphene oxide (GO), an oxidized derivative of single atomic layer graphene, possesses attractive properties such as large specific area, physiological stability, and good biocompatibility. GO contains a series of polar group including hydroxyl, carboxyl, epoxy and carbonyl groups [32, 33]. Polydopamine (PDA) as an excellent functional material has been extensively used in the fields of surface modification, drug delivery, theranostic application and so on [34, 35]. Herein, PDA was selected for surface modification of GO via oxidative polymerization of dopamine since it has good biocompatibility, biodegradability and dispersibility. Moreover, the process of PDA and proteins conjugation is speedy, simple without requiring any activation procedure. On account of the beneficial characteristics, we chose the PDA-rGO as a substrate material to immobilize a large amount of Ab₁.

According to reports the redox-potentials of platinum and iridium are respectively higher than other metallic elements (Pt²⁺ / Pt 1.19 V, Ir³⁺ / Ir 1.16 V), demonstrating the catalytic activity of Ir NPs is comparable to reported Pt nanoparticles [36]. Herein, Ir NPs were adopted to fabricate immunosensor for the detection of tumor biomarker by virtue of the inherited high catalytic activity.

Characterization of the PDA-rGO, PVP-Ir NPs

PDA-rGO were characterized by SEM (Fig. 1a) and FTIR (Fig. S1). It is easy to observe that PDA-rGO have papery

structure (Fig. 1a), which means that it has a large specific surface area, can immobilize higher levels of Ab₁ onto the electrode surface. Fig. S1 shows the FTIR spectra of GO and PDA-rGO further revealed the synthesis of PDA-rGO was successful. As revealed by the TEM image of Fig. 1b, PVP-Ir NPs were sphere-like nanoparticles with the average diameter of approximately 1.5 nm.

It is well known that the sensitivity of the immunosensor depends on signal amplification performance of the signal labels. Therefore, the catalytic activity of Ir NPs for the reduction of H₂O₂ was investigated. Figure 2 presents the electrochemical reduction performance of Ir NPs towards 5 mM H₂O₂. An increase of the electrochemical response was observed apparently that verifies the intrinsic catalase mimic performance of Ir NPs. Accordingly, the -0.6 V potential was determined as the operating potential for further electrochemical measurements.

Characterization of the immunosensor

An efficient detection method, electrochemical-impedance spectra (EIS) were used to characterize the property of surface-modified electrode. The EIS of each construction step of immunosensor consisted of semicircle and linear portion. The charge transfer resistance (R_{ct}) was provided by the semicircle diameter that represents for impede of the redox couple flux of the electrode surface, thus, this value would increase when each layer hindering the electron exchange was modified on the electrode [37]. Fig. S2 shows the EIS of the continuous building steps for modified electrodes, resulting in the successful construction of the immunosensor.

Table 1 In comparison with other methods for the detection of CEA

Method	Linear range [ng·mL ⁻¹]	Detection Limit [ng·mL ⁻¹]	Reference
GO/MWCNTs-COOH/Au@CeO ₂	0.05–100	20	[38]
rCu ₂ O-GO-AuNPs	0.01–4	4	[39]
Ag NCs-HRP	0.001–10	0.5	[40]
Au/Ag	0.001–50	0.3	[41]
This method	0.0005–5	0.23	This work

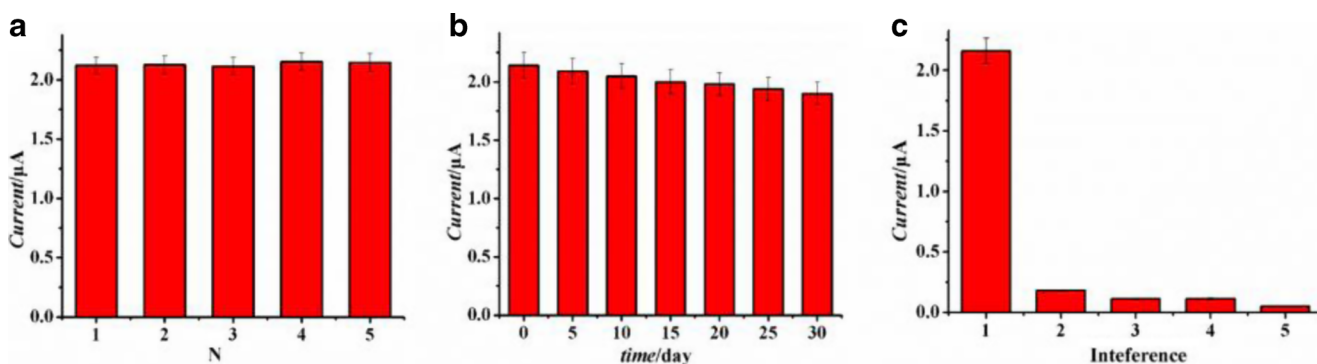


Fig. 4 **a** The current response of the immunosensors towards the same CEA concentration ($0.5 \text{ ng}\cdot\text{mL}^{-1}$); **b** The current response of the immunosensor in 30 days; **c** The current response towards $0.5 \text{ ng}\cdot\text{mL}^{-1}$ CEA, $0.5 \text{ ng}\cdot\text{mL}^{-1}$ AFP, $0.5 \text{ ng}\cdot\text{mL}^{-1}$ cTnI, $1 \text{ mg}\cdot\text{mL}^{-1}$ ascorbic acid and $1 \text{ mg}\cdot\text{mL}^{-1}$ uric acid

Analytical performance

Under the optimized conditions that is pH value of 7.4, H_2O_2 concentration of 5.0 mM, working potential of -0.6 V , PDA-rGO concentration of $1.5 \text{ mg}\cdot\text{L}^{-1}$, Ir NPs- Ab_2 concentration of $1.5 \text{ mg}\cdot\text{L}^{-1}$ as optimal operating data (shown in Fig. S3). The current change resulted from electrochemical reduction of H_2O_2 were linearly increased following the increasing concentrations of CEA (Fig. 3). Accordingly, the formula of calibration curve of CEA was $\Delta I = 0.4350 C + 2.2987$, $R = 0.99$ in the range from $0.5 \text{ pg}\cdot\text{mL}^{-1}$ to $5 \text{ ng}\cdot\text{mL}^{-1}$ with a satisfying detection limit of $0.23 \text{ pg}\cdot\text{mL}^{-1}$ ($S/N = 3$). In comparison with other CEA immunosensors, the immunosensor has more outstanding analysis performance for the CEA detection, shown in Table 1.

Reproducibility, stability and selectivity

To investigate reproducibility of the immunosensors, five modified-electrodes for the detection of $0.5 \text{ ng}\cdot\text{mL}^{-1}$ CEA were conducted, respectively. The relative standard deviation (RSD) was 1.61%, verifying the fabricated immunosensor has admirable reproducibility (Fig. 4a).

The stability of the immunosensor was proved by measuring the current response once every 5 days. The unused electrode was stored in 4°C until the next electrochemical measurement. As shown in Fig. 4b, we can see that no obvious current decline in the detection of the same electrode, and 88.7% of the initial current was remained after 30 days. Therefore, the stability was confirmed to be acceptable.

Figure 4 c exhibited the selectivity of the constructed immunosensor under the same operating conditions. Experiments were performed using $0.5 \text{ ng}\cdot\text{mL}^{-1}$ CEA, $0.5 \text{ ng}\cdot\text{mL}^{-1}$ alpha fetoprotein (AFP), $0.5 \text{ ng}\cdot\text{mL}^{-1}$ cardiac troponin I (cTnI), $1 \text{ mg}\cdot\text{mL}^{-1}$ ascorbic acid and $1 \text{ mg}\cdot\text{mL}^{-1}$ uric acid as analytical substrate, respectively. It can be seen that a considerable current signals were observed for CEA, whereas the response signals of other tumor biomarkers and interfering species were almost negligible. Thus, this

immunoassay method for detecting CEA has satisfactory capacity of anti-interference.

Analysis of human serum sample

The reliability of analytical performance and practical value of the immunosensor was confirmed through real human serum detection. The concentration of CEA in serum sample was investigated via the commercial ELISA kits. The consequence was listed in Table 2, the RSDs were respectively 4.9%, 2.5%, 1.3%, 2.5% and 1.5% at the addition of 0.5, 1, 2, 3, 4 $\text{ng}\cdot\text{mL}^{-1}$, respectively, and the recovery range from 99% to 100.5%. Thus, such immunoassay can be used to detect CEA and even other tumor biomarkers in clinical diagnosis.

Conclusion

We fabricated a sandwich electrochemical immunosensor used Ir NPs as electrochemical signal amplifier and PDA-rGO as substrate material for the detection of CEA. On account of the wide linear range, the low detection limit as well as the satisfactory reproducibility, stability and selectivity of the immunosensor, it can be attempted to use in the practical clinical analysis for patients, and also use in combination with other analytical techniques. Furthermore, this immunoassay provides good promising for the detection of tumor biomarkers beyond CEA in human serum.

Table 2 Application of the propose immunosensors in human serum

Sample [$\text{ng}\cdot\text{mL}^{-1}$]	Addition [$\text{ng}\cdot\text{mL}^{-1}$]	Found [$\text{ng}\cdot\text{mL}^{-1}$]	RSD [%, $n = 5$]	Recovery [%]
0.5	0.5	1 ± 0.05	4.9	99
0.5	1	1.5 ± 0.04	2.5	100.5
0.5	2	2.5 ± 0.05	1.3	100.2
0.5	3	3.5 ± 0.04	2.5	99.7
0.5	4	4.5 ± 0.11	1.5	99.6

Compliance with ethical standards We declare that we have no competing interests.

References

- Letilovic T, Vrhovac R, Verstovsek R, Jaksic R, Ferrajoli A (2006) Role of angiogenesis in chronic lymphocytic leukemia. *Cancer* 107(11):925–934
- Lin JH, Zhang HH, Niu SY (2015) Simultaneous determination of carcinoembryonic antigen and α -fetoprotein using an ITO immunoelectrode modified with gold nanoparticles and mesoporous silica. *Microchim Acta* 182(3–4):719–726
- Xu TS, Li XY, Zhao HX, Li XG, Zhang HY (2015) Poly(o-phenylenediamine) nanosphere-conjugated capture antibody immobilized on a glassy carbon electrode for electrochemical immunoassay of carcinoembryonic antigen. *Microchim Acta* 182(15–16):2541–2549
- Li C, Yang CY, Wu D, Li TQ, Yin YM, Li GX (2016) Improvement of enzyme-linked immunosorbent assay for the multicolor detection of biomarkers. *Chem Sci* 7(5):3011–3016
- Zhang Y, Lu F, Yan ZQ, Wu D, Ma HM, Du B, Wei Q (2015) Electrochemiluminescence immunosensing strategy based on the use of Au@Ag nanorods as a peroxidase mimic and NH_4CoPO_4 as a supercapacitive supporter: application to the determination of carcinoembryonic antigen. *Microchim Acta* 182(7–8):1421–1429
- Kuroki M, Yamaguchi A, Koga Y, Matsuoka Y (1983) Antigenic reactivities of purified preparations of carcinoembryonic antigen (CEA) and related normal antigens using four different radioimmunoassay systems for CEA. *J Immunol Methods* 60(1–2):221–233
- Feng DX, Lu XC, Dong X, Ling YY, Zhang YZ (2013) Label-free electrochemical immunosensor for the carcinoembryonic antigen using a glassy carbon electrode modified with electrodeposited Prussian blue, a graphene and carbon nanotube assembly and an antibody immobilized on gold nanoparticles. *Microchim Acta* 180(9–10):767–774
- Ilkhani H, Sarparast M, Noori A, Bathaie SZ, Mousavi MF (2015) Electrochemical aptamer/antibody based sandwich immunosensor for the detection of EGFR, a cancer biomarker, using gold nanoparticles as a signaling probe. *Biosens Bioelectron* 74:491–497
- Tang J, Tang DP, Niessner R, Chen G, Knopp D (2011) Magneto-controlled graphene immunosensing platform for simultaneous multiplexed electrochemical immunoassay using distinguishable signal tags. *Anal Chem* 83(13):5407–5414
- Tang J, Tang DP (2015) Non-enzymatic electrochemical immunoassay using noble metal nanoparticles: a review. *Microchim Acta* 182(13–14):2077–2089
- Sun XC, Lei C, Guo L, Zhou Y (2016) Giant magneto-resistance based immunoassay for the tumor marker carcinoembryonic antigen. *Microchim Acta* 183(3):1107–1114
- Ye RF, Zhu CZ, Song Y, Liu Q, Ge XX, Yang X, Zhu MJ, Du D, Li H, Lin YH (2016) Bioinspired synthesis of all-in-one organic-inorganic hybrid Nanoflowers combined with a handheld pH meter for on-site detection of food pathogen. *Small* 12(23):3094–3100
- Wei Q, Zhao YF, Du B, Wu D, Cai YY, Mao KX, Li H, Xu CX (2011) Nanoporous PtRu alloy enhanced nonenzymatic immunosensor for ultrasensitive detection of microcystin-LR. *Adv Funct Mater* 21(21):4193–4198
- Zhao Y, Zheng YQ, Kong RM, Xiao L, Qu FL (2016) Ultrasensitive electrochemical immunosensor based on horseradish peroxidase (HRP)-loaded silica-poly(acrylic acid) brushes for protein biomarker detection. *Biosens Bioelectron* 75:383–388
- Garcinuño B, Ojeda I, Moreno-Guzmán M, González-Cortés A, Yáñez-Sedeño P, Pingarrón JM (2014) Amperometric immunosensor for the determination of ceruloplasmin in human serum and urine based on covalent binding to carbon nanotubes-modified screen-printed electrodes. *Talanta* 118:61–67
- Gao ZD, Guan FF, Li CY, Liu HF, Song YY (2013) Signal-amplified platform for electrochemical immunosensor based on TiO_2 nanotube arrays using a HRP tagged antibody-Au nanoparticles as probe. *Biosens Bioelectron* 41:771–775
- Wang CC, Ding L, Qu FL (2013) Sensitive electrochemical immunosensor for platelet-derived growth factor in serum with electron transfer mediated by gold nanoparticles initiated silver enhancement. *Measurement* 46(1):279–283
- Jiang LP, Han J, Li FY, Gao J, Li YY, Dong YH, Wei Q (2015) A sandwich-type electrochemical immunosensor based on multiple signal amplification for α -fetoprotein labeled by platinum hybrid multiwalled carbon nanotubes adhered copper oxide. *Electrochim Acta* 160:7–14
- Yang ZH, Zhuo Y, Yuan R, Chai YQ (2015) An amplified electrochemical immunosensor based on in situ-produced 1-naphthol as electroactive substance and graphene oxide and Pt nanoparticles functionalized CeO_2 nanocomposites as signal enhancer. *Biosens Bioelectron* 69:321–327
- Kerman K, Saito M, Tamiya E, Yamamura S, Takamura Y (2008) Nanomaterial-based electrochemical biosensors for medical applications. *TrAC Trends Anal Chem* 27(7):585–592
- Zhao Y, Zheng YQ, Zhao CY, You JM, Qu FL (2015) Hollow PDA-Au nanoparticles-enabled signal amplification for sensitive nonenzymatic colorimetric immunodetection of carbohydrate antigen 125. *Biosens Bioelectron* 71:200–206
- Zhu C, Yang G, Li H, Du D, Lin Y (2015) Electrochemical sensors and biosensors based on nanomaterials and nanostructures. *Anal Chem* 87(1):230–249
- Mani V, Chikkaveeraiah BV, Patel V, Gutkind JS, Rusling JF (2009) Ultrasensitive immunosensor for cancer biomarker proteins using gold nanoparticle film electrodes and Multienzyme-particle amplification. *ACS Nano* 3(3):585–594
- Huo X, Liu P, Zhu J, Liu X, Ju H (2016) Electrochemical immunosensor constructed using TiO_2 nanotubes as immobilization scaffold and tracing tag. *Biosens Bioelectron* 85:698–706
- Ma X, Jia J, Cao R, Wang X, Fei H (2014) Histidine-iridium (III) coordination-based peptide Luminogenic cyclization and Cyclo-RGD peptides for cancer-cell targeting. *J Am Chem Soc* 136(51):17734–17737
- Samanta C (2008) Direct synthesis of hydrogen peroxide from hydrogen and oxygen: an overview of recent developments in the process. *Appl Catal A Gen* 350(2):133–149
- DeRosa MC, Hodgson DJ, Enright GD, Dawson B, Evans CE, Crutchley RJ (2004) Iridium luminophore complexes for unimolecular oxygen sensors. *J Am Chem Soc* 126(24):7619–7626
- Kundu S, Liang H (2011) Shape-selective formation and characterization of catalytically active iridium nanoparticles. *J Colloid Interface Sci* 354(2):597–606
- Özkar S, Finke RG (2005) Iridium (0) nanocluster, acid-assisted catalysis of neat acetone hydrogenation at room temperature: exceptional activity, catalyst lifetime, and selectivity at complete conversion. *J Am Chem Soc* 127(13):4800–4808
- Hu WH, He GL, Zhang HH, Wu XS, Li JL, Zhao ZL, Qiao Y, Lu ZS, Liu Y, Li CM (2014) Polydopamine-functionalization of graphene oxide to enable dual signal amplification for sensitive surface plasmon resonance imaging detection of biomarker. *Anal Chem* 86(9):4488–4493
- Su H, Liu DD, Zhao M, Hu WL, Xue SS, Cao Q, Le XY, Ji LN, Mao ZW (2015) Dual-enzyme characteristics of Polyvinylpyrrolidone-capped iridium nanoparticles and their cellular protective effect against H_2O_2 -induced oxidative damage. *ACS Appl Mater Interfaces* 7(15):8233–8242

32. Du D, Wang LM, Shao YY, Wang J, Engelhard MH, Lin YH (2011) Functionalized graphene oxide as a Nanocarrier in a Multienzyme labeling amplification strategy for ultrasensitive electrochemical immunoassay of phosphorylated p53 (S392). *Anal Chem* 83(3):746–752
33. Liu GD, Shen H, Mao JN, Zhang LM, Jiang Z, Sun T, Lan Q, Zhang ZJ (2013) Transferrin modified graphene oxide for Glioma-targeted drug delivery: in vitro and in vivo evaluations. *ACS Appl Mater Interfaces* 5(15):6909–6914
34. Chang DF, Gao YF, Wang LJ, Liu G, Chen YH, Wang T, Tao W, Mei L, Huang LQ, Zeng XW (2016) Polydopamine-based surface modification of mesoporous silica nanoparticles as pH-sensitive drug delivery vehicles for cancer therapy. *J Colloid Interface Sci* 463:279–287
35. Jiang L, Jiang SS, Lin YB, Yang H, Xie ZH, Lin YB, Long H (2015) Controllable synthesis of polydopamine nanoparticles in microemulsions with pH-activatable properties for cancer detection and treatment. *J Mater Chem B* 3(33):6731–6739
36. Yang T, Ma YX, Huang QL, Cao GJ, Wan S, Li N, Zhao H, Sun X, Yin FJ (2015) Palladium-iridium nanowires for enhancement of electro-catalytic activity towards oxygen reduction reaction. *Electrochem Commun* 59:95–99
37. Nassef HM, Civit L, Fragoso A, O'Sullivan CK (2009) Amperometric immunosensor for detection of celiac disease toxic gliadin based on fab fragments. *Anal Chem* 81(13):5299–5307
38. Pang XH, Li JX, Zhao YB, Wu D, Zhang Y, Du B, Ma HM, Wei Q (2015) Label-free Electrochemiluminescent immunosensor for detection of carcinoembryonic antigen based on nanocomposites of GO/MWCNTs-COOH/Au@CeO₂. *ACS Appl Mater Interfaces* 7(34). doi:10.1021/acsami.5b05185
39. Feng T, Chen X, Qiao X, Sun Z, Wang H, Qi Y, Hong C (2015) Graphene oxide supported rhombic dodecahedral Cu₂O nanocrystals for the detection of carcinoembryonic antigen. *Anal Biochem* 494:101–107
40. Quan H, Zuo CH, Li T, Liu YT, Li MY, Zhong M, Zhang YY, Qi HZ, Yang MH (2015) Electrochemical detection of carcinoembryonic antigen based on silver nanocluster/horseradish peroxidase nanocomposite as signal probe. *Electrochim Acta* 176:893–897
41. Sun GQ, Ding YN, Ma C, Zhang Y, Ge SG, Yu JH, Song XR (2014) Paper-based electrochemical immunosensor for carcinoembryonic antigen based on three dimensional flower-like gold electrode and gold-silver bimetallic nanoparticles. *Electrochim Acta* 147:650–656